NeuroImage: Clinical 23 (2019) 101851

Contents lists available at ScienceDirect

NeuroImage: Clinical

journal homepage: www.elsevier.com/locate/ynicl

Linked anatomical and functional brain alterations in children with attention-deficit/hyperactivity disorder

Zhao-Min Wu[a,b,c,d,e,*,1], Alberto Llera[e,1], Martine Hoogman[d,e], Qing-Jiu Cao[b,c], Marcel P. Zwiers[e], Janita Bralten[d,e], Li An[b,c], Li Sun[b,c], Li Yang[b,c], Bin-Rang Yang[a], Yu-Feng Zang[f], Barbara Franke[d,e,g], Christian F. Beckmann[e,2], Maarten Mennes[e,2], Yu-Feng Wang[b,c,**,2]

[a] Shenzhen Children's Hospital, China
[b] Peking University Sixth Hospital, Institute of Mental Health, National Clinical Research Center for Mental Disorders, Peking University Sixth Hospital, Beijing 100191, China
[c] Key Laboratory of Mental Health, Ministry of Health, Peking University, Beijing 100191, China
[d] Department of Human Genetics, Radboud University Medical Center, Nijmegen, the Netherlands
[e] Donders Institute for Brain, Cognition and Behavior, Nijmegen, the Netherlands
[f] Center for Cognition and Brain Disorders and the Affiliated Hospital, Hangzhou Normal University; Zhejiang Key Laboratory for Research in Assessment of Cognitive Impairments, Hangzhou, China
[g] Department of Psychiatry, Donders Institute for Brain, Cognition and Behaviour, Radboud University Medical Center, Nijmegen, the Netherlands

A B S T R A C T

Objectives: Neuroimaging studies have independently demonstrated brain anatomical and functional impairments in participants with ADHD. The aim of the current study was to explore the relationship between structural and functional brain alterations in ADHD through an integrated analysis of multimodal neuroimaging data.

Methods: We performed a multimodal analysis to integrate resting-state functional magnetic resonance imaging (MRI), structural MRI, and diffusion-weighted imaging data in a large, single-site sample of children with and without diagnosis for ADHD. The inferred subject contributions were fed into regression models to investigate the relationships between diagnosis, symptom severity, gender, and age.

Results: Compared with controls, children with ADHD diagnosis showed altered white matter microstructure in widespread white matter fiber tracts as well as greater gray matter volume (GMV) in bilateral frontal regions, smaller GMV in posterior regions, and altered functional connectivity (FC) in default mode and fronto-parietal networks. Age-related growth of GMV of bilateral occipital lobe, FC in frontal regions as well as age-related decline of GMV in medial regions seen in controls appeared reversed in children with ADHD. In the whole group, higher symptom severity was related to smaller GMV in widespread regions in bilateral frontal, parietal, and temporal lobes, as well as greater GMV in intracalcarine and temporal cortices.

Conclusions: Through a multimodal analysis approach we show that structural and functional alterations in brain regions known to be altered in subjects with ADHD from unimodal studies are linked across modalities. The brain alterations were related to clinical features of ADHD, including disorder status, age, and symptom severity.

1. Introduction §

Attention-deficit/hyperactivity disorder, ADHD, is a neurodevelopmental disorder manifesting in symptoms of inattention and/or hyperactivity and impulsiveness. It presents with substantial heterogeneity in terms of etiology, clinical presentation, and brain alterations (Tarver et al., 2014). Various neuroimaging studies have explored the neural features of subjects with ADHD by means of magnetic resonance imaging (MRI) techniques, e.g. using structural MRI (sMRI), functional MRI (fMRI), or diffusion-weighted imaging (DWI). Most consistent findings from these studies were for ADHD-related alterations in brain volume, functional connectivity (FC), and white matter microstructure in frontal and subcortical regions(Thapar and Cooper, 2016; Rubia et al., 2014; Cortese et al., 2016; Chen et al., 2016; Norman et al., 2016).

Since structural and functional features were investigated separately in most MRI studies so far, the relationships between structural and functional alterations in ADHD remain poorly understood. In the past

* Correspondence to: Zhao-Min Wu, Shenzhen Children's Hospital, China.
** Correspondence to: Yu-Feng Wang, Peking University Sixth Hospital, China.
E-mail addresses: zhaomin.wu@foxmail.com (Z.-M. Wu), wangyf@bjmu.edu.cn (Y.-F. Wang).
[1] These authors contribute equally.
[2] Shared final responsibility.

https://doi.org/10.1016/j.nicl.2019.101851
Received 29 September 2018; Received in revised form 24 April 2019; Accepted 2 May 2019
Available online 04 May 2019

decade, multimodal neuroimaging studies emerged in an attempt to aggregate different measurements. Initially, correlation tests were performed between features independently identified in different modalities(Casey et al., 2007), requiring pre-defined regions and neuroimaging features. Hypothesis-free, data-driven methods able to integrate different modalities and inform about the integration of related features are now becoming more popular. In a study using Non-negative matrix factorization(Anderson et al., 2014), an analysis integrating fMRI and sMRI information revealed co-occurring anatomical and functional features in the default mode network (DMN) to be linked to the ADHD inattentive subtype. Another analysis(Kessler et al., 2014) of gray and white matter morphometry and the whole brain functional connectome revealed that subjects with ADHD showed reduced DMN task-positive network segregation along with structural abnormalities in dorsolateral prefrontal cortex and anterior cingulate cortex. In addition, altered intra-network connectivity in DMN, dorsal attention network, and visual network along with distributed structural alterations were seen in this analysis.

In most of the previous multimodal studies, neural correlates were identified by investigating categorical case-control differences. However, given that ADHD symptoms are viewed as a dimensional, quantitative continuum in the population(Lubke et al., 2009), investigating dimensional multimodal neuroimaging alterations can provide more insight into the neural correlates of ADHD symptoms. Dimensional effects were explored before in resting state functional connectivity and white matter microstructure. Relationships between symptom severity and functional connectivity were observed for e.g. dorsal attention network (DA), default mode network (DM), salience processing network (SAL), and executive control network (CON)(Elton et al., 2014). Positive association of ADHD symptom counts with FA in widespread brain regions has been demonstrated(van Ewijk et al., 2014; Wu et al., 2017). Integrating structural and diffusion-weighted MRI revealed smaller prefrontal volumes co-occurring with abnormal white matter density in prefrontal cortex, and smaller orbitofrontal volume co-occurring with abnormalities in insula, occipital, and somato-sensory surface areas in subjects with more severe ADHD symptoms(Francx et al., 2016).

ADHD is a lifelong neurodevelopmental disorder, and the clinical symptoms of ADHD are not static. Inattentive symptoms are more stable over the lifespan than hyperactive/impulsive symptoms, which tend to wane with increasing age(Arnold et al., 2014; Semeijn et al., 2016). Although age was always added as covariate in previous studies, the interactions between age and diagnosis have seldom been explored (Schweren et al., 2016). Brain volume alterations in children with ADHD compared to typically developing children were reported in multiple studies, and findings have survived in meta- and mega-analysis (Rubia et al., 2014; Norman et al., 2016; Hoogman et al., 2017). Nevertheless, these volume alterations seem to diminish in adulthood (Onnink et al., 2014; Frodl and Skokauskas, 2012).In meta-analysis, age effects were explored on inhibition task-based fMRI, showing that supplementary motor area and basal ganglia were underactivated solely in children with ADHD relative to controls, while inferior frontal cortex and thalamus were underactivated solely in adults with ADHD(Hart et al., 2013). Significant and specific maturational lag in connections within DMN and in DMN interconnections with two task-positive networks, fronto-parietal network and ventral attention network, were also observed in ADHD. Furthermore, ADHD patients without any comorbidity were revealed to lack significant age-related changes in gray matter and white matter microstructure that were globally observed in controls(Adisetiyo et al., 2014).

In order to better understand the complex relationships between the single-modality findings, in the current study, we performed integrative, multimodal analyses of structural, functional, and diffusion-weighted MRI data in ADHD patients and healthy controls. We aimed to unravel co-segregating structural-functional alterations in ADHD by using the linked independent component analysis (FLICA) model(Smith et al., 2004; Groves et al., 2011; Groves et al., 2012). Previously, FLICA was evaluated on simulated multimodal data sets, as well as on a real data set of Alzheimer's patients and age-matched controls; this demonstrated improvements compared to alternative strategies to incorporate ICA in detecting and isolating single-modality structured noise, as well as improved accuracy in subject-course and spatial map estimates(Groves et al., 2011; Groves et al., 2012). With FLICA, we are able to extract components across multiple imaging measures that share the same across-subject variation. Previously, FLICA was only used in integrating structural and diffusion MRI. Here, we include for the first-time functional MRI, since cognitive-domain dissociated complex multisystem impairments also play an important role in the etiology and pathophysiology of ADHD. With our approach, we aimed to get insight into the integration of the structural and functional brain alterations associated with behavioral symptoms and other clinical features related to ADHD. We hypothesized that subjects with ADHD would present structural and functional synchronized alterations compared to healthy controls. To account for dimensional nature of ADHD symptoms(Lubke et al., 2009) and the dynamic clinical presentations of ADHD, we also investigated the neural correlates of symptom severity and age.

2. Methods

2.1. Participants and data acquisition

In the current study, we included data of 199 individuals (80 children with ADHD and 119 healthy controls, age-range 8–15 years), all with a right hand dominance(Oldfield, 1971). All ADHD probands were recruited from child psychiatric clinics at Peking University Sixth Hospital/Institute of Mental Health. The diagnosis of ADHD and/or other psychiatric disorders was made by clinicians with a clinical interview and a semi-structured interview based on the Schedule for Affective Disorders and Schizophrenia for School-Age Children-Present and Lifetime version (K-SADS-PL)(Kaufman et al., 1997). In addition to the interviews, the ADHD rating scale-IV (Dupaul et al., 1998) was applied providing quantitative measures of hyperactivity/impulsivity and inattention symptoms. The parent who knew the child best was regarded as the primary informant. Exclusion criteria for the ADHD group were 1) a diagnosis of schizophrenia, affective disorder, Tourette syndrome, pervasive developmental disorder, or intellectual disability; 2) history of head injury with loss of consciousness; 3) neurological abnormalities; 4) drug or substance abuse; 5) a full-scale IQ below 80. For the healthy controls, any evidence of current or past major psychiatric disorders in the K-SADS-PL assessment and/or the presence of neurological disorders lead to exclusion. Additionally, visible abnormalities (e.g., enlargement of ventricle) on the magnetic resonance images, which were examined by an experienced radiologist, lead to exclusion of cases and controls ($N = 2$, one from the ADHD group).

A battery of MRI assessments was applied, comprising structural T1 MRI (sMRI), resting state functional MRI (RS-fMRI), and diffusion-weighted imaging (DWI). Details about scanning protocols and information of the clinical battery can be found in the Supplementary Material (Methods) and Table S1. This work was approved by the Ethics committee of Peking University Health Science Center. Informed consent was obtained from parents of children prior to the study.

2.2. Preparation of DWI data using tract-based spatial statistics (TBSS)

Preprocessing steps were reported in a previous publication from our group(Wu et al., 2017). Briefly, the diffusion-weighted images of each subject were realigned on the unweighted image using mutual information routines from SPM8 (http://www.fil.ion.ucl.ac.uk/spm/software/spm8/). Next, an iteratively reweighted-least-squares algorithm (PATCH) was used to robustly correct for head and cardiac motion artifacts in the diffusion-weighted data(Zwiers, 2010). Later,

DTIFIT from the FMRIB's Diffusion Toolbox(Jenkinson et al., 2012) was used to create fractional anisotropy (FA), mean diffusivity (MD), radial diffusivity (RD), and mode of anisotropy (MO) images independently per participant. These were fed into the TBSS pipeline(Smith et al., 2006) using a sample-specific template obtained from 15 ADHD and 21 healthy control participants, who showed the highest image quality. Finally, the individual images were mapped onto the created skeleton resulting in skeletonized FA, RD, MD, and MO images for each individual.

2.3. Preparation of RS-fMRI data using independent component analysis (ICA)

The RS-fMRI data was preprocessed using FSL (http://fsl.fmrib.ox.ac.uk/fsl). Details can be found in the Supplementary Methods. Resting state networks (RSNs) were obtained via group independent component analysis (ICA)(Beckmann and Smith, 2004; Beckmann et al., 2005; Beckmann and Smith, 2005). Functional connectivity (FC) patterns of each participant that corresponded to each group independent component were obtained using a dual-regression approach(Filippini et al., 2009; Nickerson et al., 2017). Twelve components from the group ICA showed high spatial correspondence ($r > 0.4$) with the ten resting-state networks as extracted by Smith et al.(Smith et al., 2009). These components were selected for the linked ICA.

2.4. Preparation of sMRI data

The sMRI data were preprocessed using FSL voxel-based morphometry (VBM) pipeline (http://fsl.fmrib.ox.ac.uk/fsl/fslwiki/FSLVBM). Briefly, brain extraction was conducted, and a study-specific gray matter template was created from the gray matter tissue probability maps of the same individuals used to create the DWI skeleton template. Afterwards, each participant's gray matter images were registered to the template and modulated. The segmented images were then smoothed with an isotropic Gaussian kernel with a sigma of 4 mm (FWHM = 9.4 mm). Quality assurance was done by checking the slice view of each participant.

Spatial down-sampling was applied to all modalities for computational reasons(Groves et al., 2012). The voxel-based morphometry and independent component images from RS-fMRI were down-sampled to 4 mm isotropic voxels while the DTI images were down-sampled to 2 mm isotropic.

2.5. Linked ICA

Linked ICA(Groves et al., 2011) is a Bayesian multi-modal extension to the common ICA algorithm. While most ICA algorithms perform time-series factorizations, the Linked ICA algorithm provides a factorization of 'subject-series' into a set of spatially independent sources and a vector of subject contributions per source. Such 'subject-course' reflects the extent to which each subject contributes to a given source of spatial variation and can be studied in relation to behavioral measures to explain for example development, behavior, or pathologies(Smith et al., 2004; Groves et al., 2011; Groves et al., 2012; Douaud et al., 2014). Further, this model can handle the simultaneous decomposition of data modalities with different spatial dimensions (number of voxels) while forcing all modalities to share the same subject-courses for each independent component. Briefly, this method makes the integration of information from different modalities possible and provides a flexible platform to model individual variation from multimodal MRI. Moreover, the original data is explained into different components that include interrelated information from different modalities, which implies underlying biological mechanism that could never be seen in unimodal studies. In this work, we included all modalities mentioned in the previous sub-sections, i.e. VBM, FA, RD, MD, MO, and RSN spatial patterns, into the linked ICA factorization. Given our sample size and following the approach published before(Groves et al., 2011), we extracted 50 independent components. For visualization, the spatial patterns were converted to pseudo-*Z*-statistics by accounting for the scaling of the variables and the signal to noise ratio in that modality and are thresholded at $|Z| > 2.3$ for visualization purposes. Component selection was then performed based on single modality and single subject contributions to the variance in each component. More precisely, all components for which a single modality contributed > 50%, or where a single subject contributed > 10%, was excluded. This resulted in a selection of 29 components that were included in further analyses.

2.6. Statistical analysis

All subsequent statistical analyses were performed on the subject loading vectors of each selected independent component resulting from the linked ICA, as they reflect the extent to which the component is expressed in that participant's brain anatomical or FC patterns. Regression models were built and estimated using R (https://www.r-project.org/). Continuous predictors were demeaned to reduce the effect on variance inflation factor (VIF) brought by modeling interactions. To eliminate unnecessary covariance and/or redundancies among the independent variables, variable selection was done to optimize the predictors in the regression model using MASS package by exact Akaike information criterion (AIC). The original model included all possible variables, and AIC model selection was performed in both directions (forward and backward) until the model with the lowest AIC was found.

First, we studied the relation between each independent component's subject loadings and the ADHD diagnosis while simultaneously considering age, sex, scanning protocol, as well as two- and three-way interactions between diagnosis, age, and sex (see the formula for Y1 in Supplementary Material). After variable selection via AIC, all predictors remaining in the model were estimated. In cases where a significant categorical effect was found (statistically significant after Bonferroni correction across all 29 component maps), the symptom severity (total score from ADHD-RS) was added to the final model, and the categorical effect was again estimated to test the independence of categorical and dimensional effects.

Secondly, we explored ADHD symptom severity-related multimodal variations. In this case, we added to the previous model the ADHD-RS total score as well as its interaction with diagnosis (see the formula of Y2 in Supplementary Methods).

Although IQ was not included in the model, we conducted a post-hoc analysis with IQ included to eliminate the potential effect brought by different IQ in the two subject groups.

3. Results

3.1. Demographic, clinical, and cognitive measures

There were no statistically significant differences in the average age of participants in the ADHD and in the control group. The ADHD group had fewer female participants, and subjects in this group had a lower IQ. As expected, subjects with ADHD showed higher symptom scores on the ADHD-RS. Characteristics of participants are summarized in Table 1.

The relative contribution of each imaging modality to each of the 50 extracted independent components is shown in **Supplementary Fig. S1**. Out of the 50 components, 31 components spanned multiple modalities, with no single modality contributing > 50%. Based on this threshold, the other 19 components were excluded from subsequent analyses. Two additional components were excluded, since over 10% of the variance of these components was contributed by one single subject. This resulted in 29 multimodal independent components for further analyses; consequently, a significance threshold for posterior analyses was determined at a Bonferroni-corrected *p*-value smaller than 0.05/29 = 0.0017.

Table 1
Demographic, clinical and neuropsychological features of children with ADHD and healthy controls.

	ADHD (n = 80)	Control (n = 119)	P-value
Number of males (%)	71 (88.7%)	58 (48.7%)	< 0.001
Average age in years ± SD	10.95 ± 1.95	10.62 ± 1.82	0.2279
IQ ± SD	106.96 ± 14.37	118.64 ± 13.16	< 0.001
ADHD-RS full scale ± SD	30.17 ± 7.97	11.65 ± 6.63	< 0.001
RMD DTI[a] ± SD	0.13 ± 0.04	0.12 ± 0.03	0.2698
RMS-FD RS-fMRI[b] ± SD	0.10 ± 0.04	0.08 ± 0.04	0.0005
Comorbid ODD/CD (%)	25 (31.25)	(0)	
Comorbid Anxiety (%)	2 (2.50)	(0)	
Comorbid Tics (%)	5 (6.25)	(0)	
Medication naive (%)[c]	67 (83.75)	N (100)	

Abbreviations: SD, standard deviation; IQ, intellectual quotient; ADHD-RS, ADHD rating scale; RMD, relative motion displacement; DTI, diffusion tensor imaging; RS-fMRI, resting sate functional magnetic imaging; CD, conduct disorder; ODD, oppositional defiant disorder;

[a] RMS-FD: it is the mean of the relative displacement in six directions, which summarizes motion score during DTI scanning.

[b] RMS-FD: it is the root mean squared of the relative displacement time series, which summarizes motion score across time during scanning.

[c] The percentage of patients with no ADHD-related pharmacological treatment. history (both stimulant and non-stimulant included); All patients were medication free for at least 1 month before the MRI scan.

3.2. Anatomical and functional alterations in children with ADHD compared to healthy controls

3.2.1. Case-control differences

Component 9 (IC9) showed significant diagnosis and diagnosis by sex interaction effects (diagnosis $\beta = 1.438$, $p_{nominal} = 0.00004$, diagnosis*sex $\beta = -1.415$, $p_{nominal} = 0.00026$, sex $\beta = 0.519$, $p_{nominal} = 0.00364$). Compared with healthy controls, children with ADHD showed smaller FA, greater RD, and greater MD in white matter fiber tracts including anterior thalamic radiation, cingulum, body of corpus callosum (CC) and corticospinal tract, greater gray matter volume (GMV) in bilateral frontal regions, smaller GMV in posterior brain regions, as well as altered functional connectivity in several networks, most notably the DMN and fronto-parietal network in their nodes located in precuneus cortex and medial frontal gyrus (Fig. 1). In summary, the IC9 showed co-segregating structural and functional alterations in precuneus, as well as bilateral frontal cortex. Besides the main effects of diagnosis, interaction between diagnosis and sex was also showed in IC09. Note that, in our model, the coefficients for diagnosis and diagnosis*sex were 1.437 and − 1.415, which means that the effect of diagnosis remained positive independent of sex (1 for male or 0 for female). Leaving the main effects of diagnosis out, in male subjects, loadings of IC9 were higher in controls than participants with ADHD ($p = 0.0412$), while a reverse relationship was found in female subjects ($p = 0.000488$). By adding the ADHD rating scale total score into the regression model, the case-control differences and diagnosis*sex effects seen in IC9 remained nominally significant ($p = 0.0198$ and 0.000234, respectively). A significant linear positive correlation was seen between subject loadings in IC9 and ADHD-RS total score (Fig. 1). Including IQ into the model did not change these results (not shown).

3.2.2. Age-related diagnosis effects

Component 37 (IC37) yielded a diagnosis-by-age interaction. Specifically, the age-related cross-sectional trajectories of IC37 were different in subjects with ADHD compared to healthy controls (diagnosis*age: $p_{nominal} = 0.00156$). As shown in the bottom panel of Fig. 2, the loading of IC37 appeared to get greater as age increases in the control group, while it appeared to get smaller as age increases in the ADHD group. IC 37 showed co-segregating functional and structural alterations in bilateral and medial frontal regions, as well as substantives structural alterations in the posterior part of the brain. In the control group, as age increased, RD and MD in the corticospinal tract and anterior thalamic radiation, as well as GMV of posterior parts of the brain become larger, including temporal and occipital lobes, while FA in bilateral anterior thalamic radiation, GMV of bilateral and medial frontal regions became smaller. FC strength also changed with age; in the control group, FC strength in nodes of the DMN located in precuneus cortex, bilateral frontal regions, and frontal pole became larger, while FC strength in medial frontal regions became smaller as age increased. In the fronto-parietal network of the control group, FC in bilateral frontal regions became larger, while FC in right fronto-parietal regions within the left fronto-parietal network (FPN) and left fronto-parietal regions within the right FPN became smaller with age; this suggested stronger within-hemisphere fronto-parietal connectivity and weaker inter-hemisphere fronto-parietal connections in adolescence compared to childhood. Lastly, in the control group, FC in nodes located in bilateral frontal regions within the executive control network (ECN) was stronger, while FC in medial frontal regions was weaker in those with higher age. All age effects described above were reversed in children with ADHD. Neither including IQ nor total ADHD symptom scores into the model changed the results (not shown).

3.3. Anatomical and functional alterations related to ADHD symptom severity

Component 35 (IC35) showed significant effects of ADHD symptom severity (ADHD-RS total score, nominal $p = .00089$) that were not related to diagnostic status. In Fig. 3, we show that higher symptom severity was related to decreased loadings of IC35, which means that with respect to controls, ADHD subjects presented smaller FA in bilateral superior longitudinal fasciculus and bilateral inferior fronto-occipital fasciculus, larger RD and MD in corticospinal tract and anterior thalamic radiation, smaller gray matter in widespread regions in bilateral frontal, parietal, and temporal lobes, larger GMV in intracalcarine cortex and bilateral temporal regions, altered functional connectivity in precuneus cortex in DMN, bilateral lateral frontal cortex in FPN, and inferior temporal and occipital cortex in auditory network. IC35, in summary, showed co-segregating wide-spread structural alterations and functional alterations, especially superior and dorsal-lateral part of the brain. Neither the correlation between diagnosis and IC35 nor the interaction between diagnosis and symptoms were significant for this component, which allowed us to merge cases and controls to cover the whole symptom spectrum. As mentioned above, a significant linear correlation was also seen between subject loadings in IC9 and ADHD-RS total score (Fig. 1).

4. Discussion

In the current study, we integrated sMRI, RS-MRI, and DWI to investigate ADHD-related alterations in the different imaging modalities and links among those as well as their relation to age and symptom severity. The current study identified co-occurring anatomical and functional alterations in ADHD: larger GMV in bilateral frontal regions, smaller GMV and larger FC in precuneus cortex, and altered white matter microstructure were found in children with ADHD compared to healthy controls. Age-related differences of GMV in healthy controls in distributed regions of the brain and FC in bilateral frontal regions were found to be reversed in children with ADHD. In both patients and healthy controls, a higher number of ADHD symptoms was accompanied by smaller GMV in bilateral frontal, parietal, and temporal lobes, larger GMV in intracalcarine and bilateral temporal cortices and altered FC in precuneus.

Most multimodal studies, including the current one, have partly replicated results from unimodal studies and further demonstrated the interrelationship of alterations seen in different modalities. Our results confirmed the altered functional connectivity in DMN and fronto-parietal network in children with ADHD seen in unimodal studies(Elton

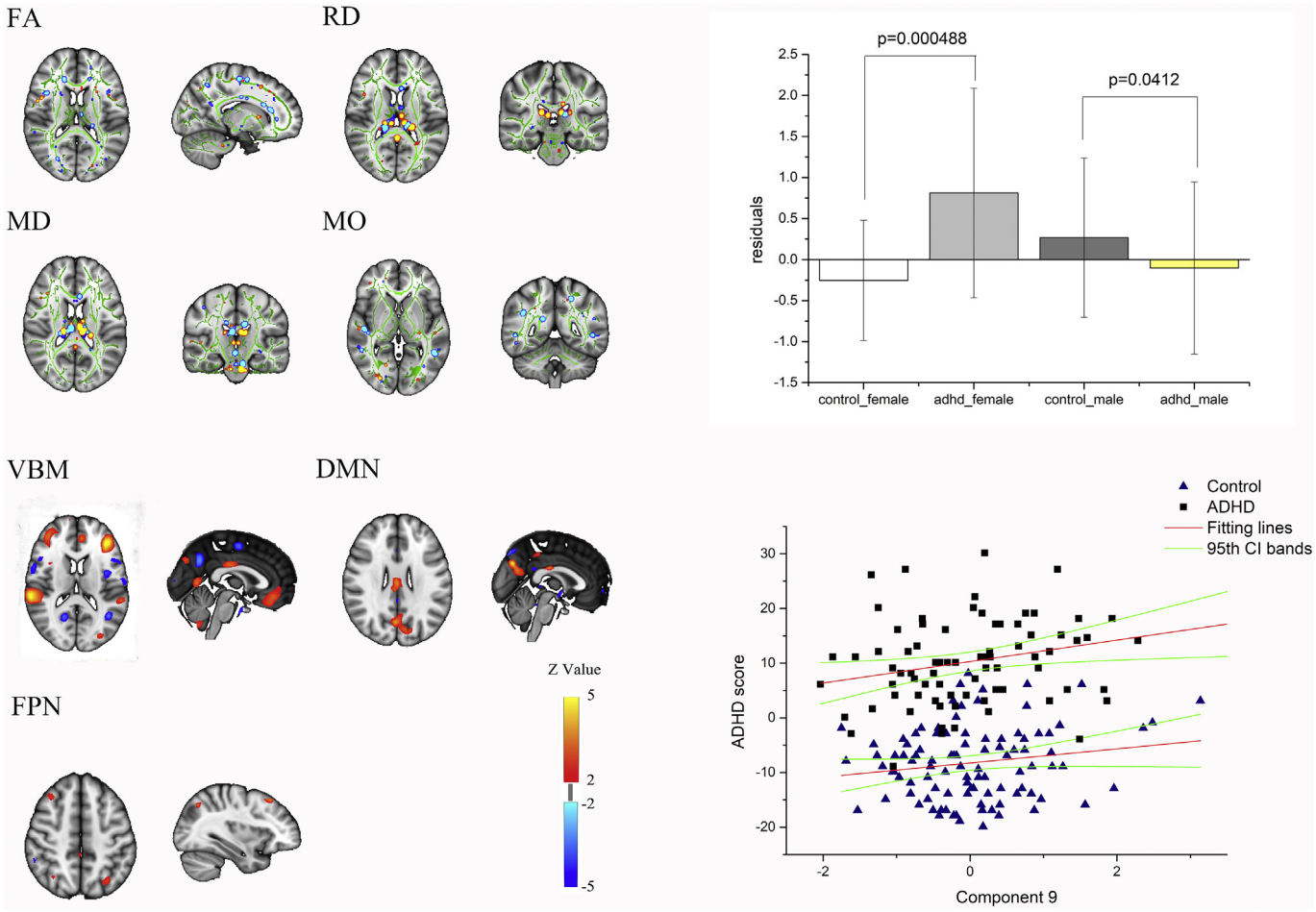

Fig. 1. Spatial representation of each modality's contribution to component 9, bar plots of subject loadings of component 9, and correlation between total ADHD symptom score and subject loadings of component 9. Note that the residuals were used in the bar plots of subject loadings of omponent9 in order to better illustrate the interaction effects. Spatial maps were thresholded at $|z| = 2.3$. Blue colors indicate negative values on this MRI measure, while red colors indicate positive values. FA = Fractional Anisotropy, RD = Radial Diffusivity, MD = Mean Diffusivity, MO = Diffusion Mode, VBM = Voxel-Based Morphometry, DMN = Default Mode Network; FPN = Frontoparietal Network. (For interpretation of the references to color in this figure legend, the reader is referred to the web version of this article.)

et al., 2014; Lin et al., 2015; Bos et al., 2017). Previous findings of smaller FA and greater RD and MD in widespread regions including anterior thalamic radiation, and cingulum and body of the corpus callosum(van Ewijk et al., 2014; Wu et al., 2017; Svatkova et al., 2016; Onnink et al., 2015; Aoki et al., 2018) (the latter FA finding also seen in meta-analysis(Chen et al., 2016)) were also replicated. Moreover, the observed GMV reduction in posterior brain regions in ADHD was also in line with some previous studies(Bralten et al., 2016; Vilgis et al., 2016; Carmona et al., 2005). However, we were not able to replicate the GMV reduction in anterior parts of the brain (Frodl and Skokauskas, 2012; Saad et al., 2017). This might be due to the fact that we used a method that can decompose brain alterations into different components, and each one probably reflects part of the effect discovered before. For example, frontal GMV alterations were present in several components. In IC9 (Fig. 1), we showed larger frontal GMV in the ADHD group and a positive correlation between symptom severity and frontal GMV. In IC35 (Fig. 3), the correlation between symptom severity and frontal GMV was reversed. In addition, frontal GMV was larger in older subjects with ADHD while it was smaller in older controls in IC37 (Fig. 2). Moreover, the sex effect (**right top of** Fig. 1) showed the complex interaction between diagnosis and sex. Although the effect of diagnosis remains positive in both sexes, the effect is mainly confined to females.

In terms of symptomatology, we showed that a higher number of ADHD symptoms was mainly accompanied by alterations of GMV in bilateral frontal, parietal, and temporal regions. Frontal and temporal gray matter, caudate, and cerebellar volumes were also previously found correlated significantly with parent- and clinician-rated severity measures in people with ADHD(Castellanos et al., 2002). Dimensional relationships between functional connectivity and symptom severity have been described for dorsal attention network, DMN, salience processing network, and executive control network(Elton et al., 2014), seen here especially for DMN for patients and controls. A higher number of ADHD symptoms was accompanied by alterations in GMV and functional connectivity, where categorical effects were not seen; since white matter alterations were not present in this component, these results may differ from previous unimodal studies(van Ewijk et al., 2014).

Demographic factors affect brain structure and function. Patients and healthy controls are known to exhibit similar back-to-front waves of brain maturation (surface area and gyrification) with different areas peaking at different times(Shaw et al., 2012). Developmental delays in brain surface area changes in subjects with ADHD have been found in prefrontal cortical regions in longitudinal assessments(Shaw et al., 2012). With the limitation that our study had a cross-sectional design, we also identified age-dependent alterations of GMV and FC in frontal regions within multiple networks, including regions found altered in ADHD in previous studies, i.e. DMN and fronto-parietal network(Rubia et al., 2014; Cortese, 2012). We found age-dependent alteration of intra-hemispheric fronto-parietal FC and decreases of inter-hemispheric fronto-parietal connection in healthy controls, while the pattern was

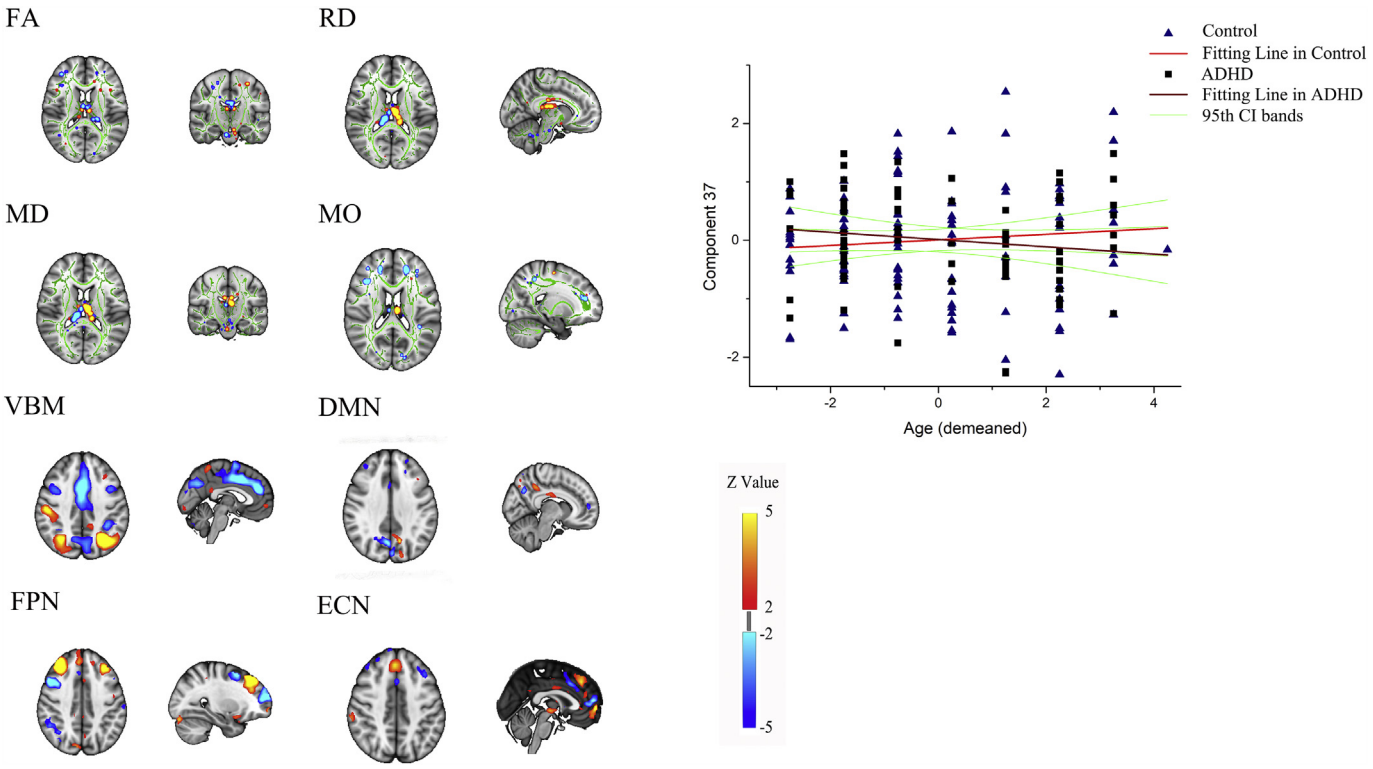

Fig. 2. Spatial representation of each modality's contribution to component 37, and correlation between age and subject loadings of component 37. Spatial maps were thresholded at $|z| = 2.3$. Blue colors indicate negative values on this MRI measure, while red colors indicate positive values. VBM = Voxel-Based Morphometry, DMN = Default Mode Network; FPN = Frontoparietal Network; ECN = Executive Control Network; Visual = Visual Network; Auditory = Auditory Network. (For interpretation of the references to color in this figure legend, the reader is referred to the web version of this article.)

opposite in subjects with ADHD. This suggests that the specificity of the developing connectome is disturbed by ADHD. Supporting this idea, the notion of "diffuse-to-focal" changes in activation patterns, simultaneous pruning of local connectivity and strengthening of long-range connectivity, and development of hemispheric specialization and lateralization with age have been suggested in multiple studies in healthy individuals(Uddin et al., 2010; Durston et al., 2006; Herve et al., 2013; Friederici et al., 2011).

Extending current knowledge by integrating different modalities, we observed that participants with ADHD show co-segregating functional and structural alterations in precuneus, including altered volume, microstructure, and functional connectivity. We also saw alterations in inter-hemisphere structural (body of corpus callosum) and functional (fronto-parietal network) connectivity, which marks interconnected structural and functional alterations. Furthermore, smaller FC in thalamus and part of the precuneus region were identified, corresponding to altered microstructure in anterior thalamic radiation, which anatomically connects the thalamus and precuneus. Nevertheless, the volumetric alterations were more widely spread than the functional alterations, and the functional alterations were more widely spread than those in white matter microstructure. Previously, in another multimodal study using the joint-ICA method9, observed alterations in macrostructure appeared more widely distributed than alterations in brain function. Using FLICA, our results now allowed a more individualized calculation of each modality compared to the joint-ICA, and enabled us to identify interconnected alterations in brain structure and function linked to the same clinical feature of ADHD. We demonstrated that the frontal region, precuneus, and the cortical-subcortical connecting fiber bundles were the most frequently affected regions. Our results in the current study show that brain alterations in children with ADHD are a combination of categorical, dimensional, and developmental effects. On top of the fundamental categorical alterations seen, symptom severity differences may make it possible that some participants with ADHD present milder brain alterations than others. The different developmental trajectory of brain function and structure might enable some participants with ADHD to 'outgrow' the disorder.

Our findings should be viewed in light of some strengths and limitations. To our knowledge, this is the first integrative analysis of structural, diffusion-weighted, and functional MRI data in a clinical ADHD cohort. By using an ICA method, we could separate brain features into independent components, and step-by-step regression models enabled us to optimize model fitting. The majority of ADHD participants in our cohort was diagnosed as 'pure ADHD', which enabled us to explore development-related changes of ADHD without being confounded by comorbidities. Our cohort had less female than male subjects, which limited our ability to explore sex effects. Medication has been demonstrated to affect brain structure and function(Spencer et al., 2013; Chou et al., 2015). Although the majority of the patients in the current study (~84%) had no history of pharmacological treatment, and all patients were medication-free for at least one month prior to scanning, we cannot rule out that medication might have had an effect on our results. Furthermore, we explored age effects in a cross-sectional cohort. While this worked well in the recent meta-analysis of brain volumes by the ENIGMA-ADHD working group(Hoogman et al., 2017), longitudinal data should be preferred to investigate multimodal developmental trajectories. Last but not least, our statistical modeling procedures bear some risk of overfitting, as we did not perform cross-validation. However, the pruning of the regression model and limiting the number of parameters in the model made overfitting less likely.

In summary, by applying Linked ICA to a cross-section clinical cohort of about 200 participants, we demonstrated linked structural and functional alterations in brain regions that individually have been demonstrated in subjects with ADHD in unimodal studies. This points to a joint underlying biological mechanism. These effects found in joint multimodal analysis indicated that they are mechanistically related as they are driven by the same subjects, which can be not clarified in

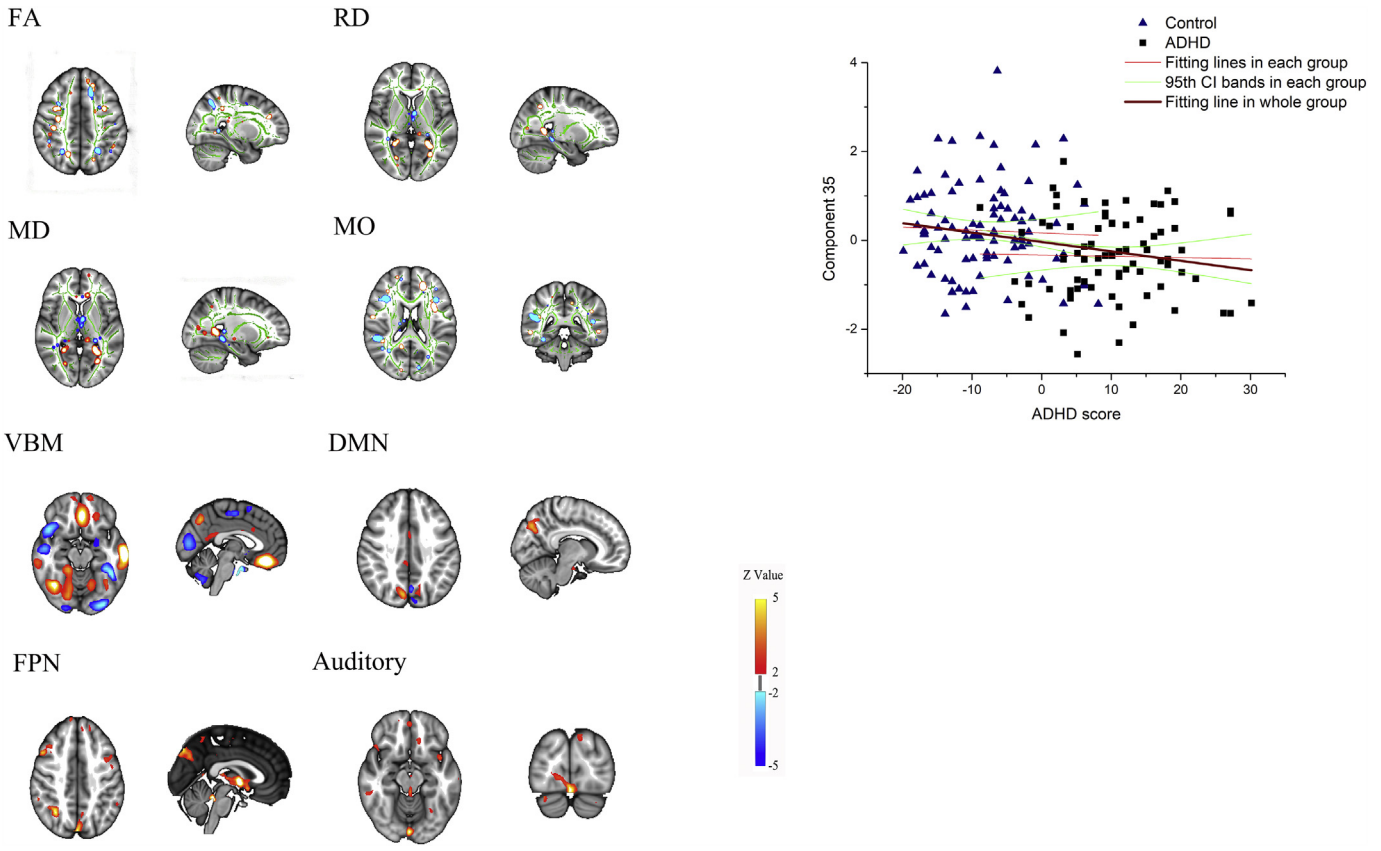

Fig. 3. Spatial representation of each modality's contribution to component 35, and correlation between total ADHD symptom score and subject loadings of component 35. Spatial maps were thresholded at $|z| = 2.3$. Blue colors indicate negative values on this MRI measure, while red colors indicate positive values. RD = Radial Diffusivity, MD = Mean Diffusivity VBM = Voxel-Based Morphometry, DMN = Default Mode Network. (For interpretation of the references to color in this figure legend, the reader is referred to the web version of this article.)

multiple unimodal analyses. The current study contributes to the ongoing exploration of multimodal brain alterations in ADHD. ADHD is a neurodevelopmental disorder, and the clinical features of ADHD patients are highly heterogeneous and change across the lifespan. Studying multiple dimensions can inform us about the different neurodevelopmental mechanisms underlying the disorder.

Disclosure

Zhao-Min Wu, Alberto Llera, Martine Hoogman, Qing-Jiu Cao, Marcel P. Zwiers, Janita Bralten, Li An, Li Sun, Li Yang, Binrang Yang, Yu-Feng Zang, Christian Beckmann, Maarten Mennes, Yu-Feng Wang do not have conflicts of interest. Barbara Franke has received educational speaking fees from Shire and Medice.

The author(s) disclosed receipt of the following financial support for the research, authorship, and/or publication of this article: This work was supported by Sanming Project of Medicine in Shenzhen "The ADHD research group from Peking University Sixth hospital" (SZSM201612036), the National Basic Research Program of China (973 program 2014CB846104, to Yu-Feng Wang), Beijing Municipal Science & Technology Commission (Z151100003915122 to Yu-Feng Wang), the National Natural Science Foundation of China (81471382, to Qing-Jiu Cao; 81371496 to Li Sun), Open Research Fund of the State Key Laboratory of Cognitive Neuroscience and Learning (CNLYB1508 to Qing-Jiu Cao), the China Scholarship Council (CSC201406010251, to Zhao-Min Wu). Martine Hoogman, Janita Bralten, and Barbara Franke are supported by a Vici grant from the Netherlands Organization for Scientific Research (NWO) (grant 016-130-669 to Barbara Franke) and by grants from the European Community's Seventh Framework Programme (FP7/2007–2013) under grant agreements n° 602,450 (IMAGEMEND) and n° 278,948 (TACTICS). Maarten Mennes was supported by a Marie Curie International Incoming Fellowship under the European Union's Seventh Framework Programme (FP7/ 2007–2013), Grant No. 327340 (Brain Fingerprint). Christian F. Beckmann gratefully acknowledges funding from the Wellcome Trust UK Strategic Award (098369/Z/12/Z). Christian F. Beckmann is also supported by the Netherlands Organization for Scientific Research (NWO-Vidi 864–12-003). This work was carried out on the Dutch national e-infrastructure with the support of SURF Cooperative.

Appendix A. Supplementary data

Supplementary data to this article can be found online at https://doi.org/10.1016/j.nicl.2019.101851.

References

Adisetiyo, V., Tabesh, A., Di Martino, A., et al., 2014. Attention-deficit/hyperactivity disorder without comorbidity is associated with distinct atypical patterns of cerebral microstructural development. Hum. Brain Mapp. 35 (5), 2148–2162.

Anderson, A., Douglas, P.K., Kerr, W.T., et al., 2014. Non-negative matrix factorization of multimodal MRI, fMRI and phenotypic data reveals differential changes in default mode subnetworks in ADHD. NeuroImage 102 (Pt 1), 207–219.

Aoki, Y., Cortese, S., Castellanos, F.X., 2018. Research review: diffusion tensor imaging studies of attention-deficit/hyperactivity disorder: meta-analyses and reflections on head motion. J. Child Psychol. Psychiatry Allied Discip. 59 (3), 193–202.

Arnold, L.E., Ganocy, S.J., Mount, K., et al., 2014. Three-year latent class trajectories of attention-deficit/hyperactivity disorder (ADHD) symptoms in a clinical sample not selected for ADHD. J. Am. Acad. Child Adolesc. Psychiatry 53 (7), 745–760.

Beckmann, C.F., Smith, S.M., 2004. Probabilistic independent component analysis for functional magnetic resonance imaging. IEEE Trans. Med. Imaging 23 (2), 137–152.

Beckmann, C.F., Smith, S.M., 2005. Tensorial extensions of independent component analysis for multisubject FMRI analysis. NeuroImage 25 (1), 294–311.

Beckmann, C.F., DeLuca, M., Devlin, J.T., Smith, S.M., 2005. Investigations into resting-

state connectivity using independent component analysis. Philos. Trans. R. Soc. Lond. Ser. B Biol. Sci. 360 (1457), 1001–1013.
Bos, D.J., Oranje, B., Achterberg, M., et al., 2017. Structural and functional connectivity in children and adolescents with and without attention deficit/hyperactivity disorder. J. Child Psychol. Psychiatry Allied Discip. 58 (7), 810–818.
Bralten, J., Greven, C.U., Franke, B., et al., 2016. Voxel-based morphometry analysis reveals frontal brain differences in participants with ADHD and their unaffected siblings. J. Psychiatry Neurosci. 41 (4), 272–279.
Carmona, S., Vilarroya, O., Bielsa, A., et al., 2005. Global and regional gray matter reductions in ADHD: a voxel-based morphometric study. Neurosci. Lett. 389 (2), 88–93.
Casey, B.J., Epstein, J.N., Buhle, J., et al., 2007. Frontostriatal connectivity and its role in cognitive control in parent-child dyads with ADHD. Am. J. Psychiatry 164 (11), 1729–1736.
Castellanos, F.X., Lee, P.P., Sharp, W., et al., 2002. Developmental trajectories of brain volume abnormalities in children and adolescents with attention-deficit/hyperactivity disorder. Jama 288 (14), 1740–1748.
Chen, L., Hu, X., Ouyang, L., et al., 2016. A systematic review and meta-analysis of tract-based spatial statistics studies regarding attention-deficit/hyperactivity disorder. Neurosci. Biobehav. Rev. 68, 838–847.
Chou, T.L., Chia, S., Shang, C.Y., Gau, S.S., 2015. Differential therapeutic effects of 12-week treatment of atomoxetine and methylphenidate on drug-naive children with attention deficit/hyperactivity disorder: a counting Stroop functional MRI study. Eur. Neuropsychopharmacol. 25 (12), 2300–2310.
Cortese, S., 2012. The neurobiology and genetics of attention-deficit/hyperactivity disorder (ADHD): what every clinician should know. Eur. J. Paediatr. Neurol. 16 (5), 422–433.
Cortese, S., Castellanos, F.X., Eickhoff, C.R., et al., 2016. Functional decoding and Meta-analytic connectivity Modeling in adult attention-deficit/hyperactivity disorder. Biol. Psychiatry 80 (12), 896–904.
Douaud, G., Groves, A.R., Tamnes, C.K., et al., 2014. A common brain network links development, aging, and vulnerability to disease. Proc. Natl. Acad. Sci. U. S. A. 111 (49), 17648–17653.
Dupaul, G.J., Power, T.J., Arthur, D., Reid, R., 1998. ADHD Rating Scale-IV: Checklists, Norms, and Clinical Interpretations. Guilford, New York.
Durston, S., Davidson, M.C., Tottenham, N., et al., 2006. A shift from diffuse to focal cortical activity with development. Dev. Sci. 9 (1), 1–8.
Elton, A., Alcauter, S., Gao, W., 2014. Network connectivity abnormality profile supports a categorical-dimensional hybrid model of ADHD. Hum. Brain Mapp. 35 (9), 4531–4543.
Filippini, N., MacIntosh, B.J., Hough, M.G., et al., 2009. Distinct patterns of brain activity in young carriers of the APOE-epsilon4 allele. Proc. Natl. Acad. Sci. U. S. A. 106 (17), 7209–7214.
Francx, W., Llera, A., Mennes, M., et al., 2016. Integrated analysis of gray and white matter alterations in attention-deficit/hyperactivity disorder. NeuroImage Clin. 11, 357–367.
Friederici, A.D., Brauer, J., Lohmann, G., 2011. Maturation of the language network: from inter- to intrahemispheric connectivities. PLoS ONE 6 (6), e20726.
Frodl, T., Skokauskas, N., 2012. Meta-analysis of structural MRI studies in children and adults with attention deficit hyperactivity disorder indicates treatment effects. Acta Psychiatr. Scand. 125 (2), 114–126.
Groves, A.R., Beckmann, C.F., Smith, S.M., Woolrich, M.W., 2011. Linked independent component analysis for multimodal data fusion. NeuroImage 54 (3), 2198–2217.
Groves, A.R., Smith, S.M., Fjell, A.M., et al., 2012. Benefits of multi-modal fusion analysis on a large-scale dataset: life-span patterns of inter-subject variability in cortical morphometry and white matter microstructure. NeuroImage 63 (1), 365–380.
Hart, H., Radua, J., Nakao, T., Mataix-Cols, D., Rubia, K., 2013. Meta-analysis of functional magnetic resonance imaging studies of inhibition and attention in attention-deficit/hyperactivity disorder: exploring task-specific, stimulant medication, and age effects. JAMA Psychiatry 70 (2), 185–198.
Herve, P.Y., Zago, L., Petit, L., Mazoyer, B., Tzourio-Mazoyer, N., 2013. Revisiting human hemispheric specialization with neuroimaging. Trends Cogn. Sci. 17 (2), 69–80.
Hoogman, M., Bralten, J., Hibar, D.P., et al., 2017. Subcortical brain volume differences in participants with attention deficit hyperactivity disorder in children and adults: a cross-sectional mega-analysis. Lancet Psychiatry 4 (4), 310–319.
Jenkinson, M., Beckmann, C.F., Behrens, T.E., Woolrich, M.W., Smith, S.M., 2012. Fsl. NeuroImage 62 (2), 782–790.
Kaufman, J., Birmaher, B., Brent, D., et al., 1997. Schedule for affective disorders and schizophrenia for school-age children-present and lifetime version (K-SADS-PL): initial reliability and validity data. J. Am. Acad. Child Adolesc. Psychiatry 36 (7), 980–988.
Kessler, D., Angstadt, M., Welsh, R.C., Sripada, C., 2014. Modality-spanning deficits in attention-deficit/hyperactivity disorder in functional networks, gray matter, and white matter. J. Neurosci. 34 (50), 16555–16566.
Lin, H.Y., Tseng, W.Y., Lai, M.C., Matsuo, K., Gau, S.S., 2015. Altered resting-state frontoparietal control network in children with attention-deficit/hyperactivity disorder. J. Int. Neuropsychol. Soc. 21 (4), 271–284.
Lubke, G.H., Hudziak, J.J., Derks, E.M., van Bijsterveldt, T.C., Boomsma, D.I., 2009. Maternal ratings of attention problems in ADHD: evidence for the existence of a continuum. J. Am. Acad. Child Adolesc. Psychiatry 48 (11), 1085–1093.
Nickerson, L.D., Smith, S.M., Ongur, D., Beckmann, C.F., 2017. Using dual regression to investigate network shape and amplitude in functional connectivity analyses. Front. Neurosci. 11, 115.
Norman, L.J., Carlisi, C., Lukito, S., et al., 2016. Structural and functional brain abnormalities in attention-deficit/hyperactivity disorder and obsessive-compulsive disorder: a comparative Meta-analysis. JAMA Psychiatry 73 (8), 815–825.
Oldfield, R.C., 1971. The assessment and analysis of handedness: the Edinburgh inventory. Neuropsychologia 9 (1), 97–113.
Onnink, A.M., Zwiers, M.P., Hoogman, M., et al., 2014. Brain alterations in adult ADHD: effects of gender, treatment and comorbid depression. Eur. Neuropsychopharmacol. 24 (3), 397–409.
Onnink, A.M., Zwiers, M.P., Hoogman, M., et al., 2015. Deviant white matter structure in adults with attention-deficit/hyperactivity disorder points to aberrant myelination and affects neuropsychological performance. Prog. Neuro-Psychopharmacol. Biol. Psychiatry 63, 14–22.
Rubia, K., Alegria, A.A., Brinson, H., 2014. Brain abnormalities in attention-deficit hyperactivity disorder: a review. Rev. Neurol. 58 (Suppl. 1), S3–S16.
Saad, J.F., Griffiths, K.R., Kohn, M.R., Clarke, S., Williams, L.M., Korgaonkar, M.S., 2017. Regional brain network organization distinguishes the combined and inattentive subtypes of attention deficit hyperactivity disorder. NeuroImage Clin. 15, 383–390.
Schweren, L.J., Hartman, C.A., Zwiers, M.P., et al., 2016. Stimulant treatment history predicts frontal-striatal structural connectivity in adolescents with attention-deficit/hyperactivity disorder. Eur. Neuropsychopharmacol. 26 (4), 674–683.
Semeijn, E.J., Comijs, H.C., de Vet, H.C., et al., 2016. Lifetime stability of ADHD symptoms in older adults. Atten. Defic. Hyperact Disord. 8 (1), 13–20.
Shaw, P., Malek, M., Watson, B., Sharp, W., Evans, A., Greenstein, D., 2012. Development of cortical surface area and gyrification in attention-deficit/hyperactivity disorder. Biol. Psychiatry 72 (3), 191–197.
Smith, S.M., Jenkinson, M., Woolrich, M.W., et al., 2004. Advances in functional and structural MR image analysis and implementation as FSL. NeuroImage 23 (Suppl. 1), S208–S219.
Smith, S.M., Jenkinson, M., Johansen-Berg, H., et al., 2006. Tract-based spatial statistics: voxelwise analysis of multi-subject diffusion data. NeuroImage 31 (4), 1487–1505.
Smith, S.M., Fox, P.T., Miller, K.L., et al., 2009. Correspondence of the brain's functional architecture during activation and rest. Proc. Natl. Acad. Sci. U. S. A. 106 (31), 13040–13045.
Spencer, T.J., Brown, A., Seidman, L.J., et al., 2013. Effect of psychostimulants on brain structure and function in ADHD: a qualitative literature review of magnetic resonance imaging-based neuroimaging studies. J. Clin. Psychiatry 74 (9), 902–917.
Svatkova, A., Nestrasil, I., Rudser, K., Goldenring Fine, J., Bledsoe, J., Semrud-Clikeman, M., 2016. Unique white matter microstructural patterns in ADHD presentations-a diffusion tensor imaging study. Hum. Brain Mapp. 37 (9), 3323–3336.
Tarver, J., Daley, D., Sayal, K., 2014. Attention-deficit hyperactivity disorder (ADHD): an updated review of the essential facts. Child Care Health Dev. 40 (6), 762–774.
Thapar, A., Cooper, M., 2016. Attention deficit hyperactivity disorder. Lancet 387 (10024), 1240–1250.
Uddin, L.Q., Supekar, K., Menon, V., 2010. Typical and atypical development of functional human brain networks: insights from resting-state FMRI. Front. Syst. Neurosci. 4, 21.
van Ewijk, H., Heslenfeld, D.J., Zwiers, M.P., et al., 2014. Different mechanisms of white matter abnormalities in attention-deficit/hyperactivity disorder: a diffusion tensor imaging study. J. Am. Acad. Child Adolesc. Psychiatry 53 (7), 790–799 (e793).
Vilgis, V., Sun, L., Chen, J., Silk, T.J., Vance, A., 2016. Global and local grey matter reductions in boys with ADHD combined type and ADHD inattentive type. Psychiatry Res. 254, 119–126.
Wu, Z.M., Bralten, J., Cao, Q.J., et al., 2017. White matter microstructural alterations in children with ADHD: categorical and dimensional perspectives. Neuropsychopharmacology 42 (2), 572–580.
Zwiers, M.P., 2010. Patching cardiac and head motion artefacts in diffusion-weighted images. NeuroImage 53 (2), 565–575.